Artificial neural network as an analyze tool for optical coherence tomography images of experimental stroke models - a pilot study

Costin Teodor Streba[1], Sabina Ligia Georgescu[2], Maria Jigău[3],
Maria Andreea Dinu[4], Tudor-Adrian Bălşeanu[1],
Venera Cristina Dinescu[1], Bogdan Cătălin[1], Eugen Osiac[1]
[1] *University of Medicine and Pharmacy of Craiova, Faculty of Medicine, 2-4 Petru Rares Str., Craiova 200349, Dolj, Romania*
[2] *National College Unirea Târgu Mureş, 17 Mihai Viteazul Str., Târgu Mureş 540080, Mureş, Romania*
[3] *University of Craiova, Faculty of Mathematics and Natural Science, Department of Physics, 13 A.I. Cuza Str., Craiova 200585, Dolj, Romania*
[4] *Clinical Emergency University Hospital of Craiova, 1 Tabaci Str., Craiova 200642, Dolj, Romania*

Abstract

This paper presents the results of testing an artificial neuronal network as automatic images analyses for optical coherence tomography investigations of brain injuries. Although optical coherence tomography is a very promising tool for many brain lesions studies, lack of statistical/mathematical models for automatic interpretation and detection could be a large inconvenient. Our setup is providing a feasible model for showing accurate detection of stroke injuries inside the frame of rodent experiments.

Keywords: optical coherence tomography, stroke, artificial neural network

1 Introduction

Optical coherence tomography (OCT) was developed as an optical method for imaging on micron resolution scale [1-3]. The method, which was introduced into medical research in the last two decades, is based on the optical concept of low coherence interference imaging [4-6] and can be considered similar with the B-mode ultrasound detection design, with the differences that is using light instead of ultrasounds. Considering its features, OCT devices are able to provide high-speed analysis, microns range resolution and non-invasive investigations of different tissues [7]. OCT was primary used for characterize structural and functional investigations in ophthalmology field [8-10] but the developments enlarge the applications area to gastroenterology [11-14], dermatology [15] and neurology [16-20], where OCT was already reported by several groups as a potential tool for brain imaging [21]. Cerebral ischemia generating stroke represents one of the most important causes of death and disability in western countries [22], but is still suffering of a lack of imaging

investigations and monitoring of injured area being under a continuous search for new technologies. Hence this kind of injury can be considered a good candidate for OCT investigations, especially due to the impossibility of physical biopsies and because the brain cortex is situated next to the skin surface. The OCT investigations of the experimental brain injuries were already implemented by our group [21, 23]. In our previous experiments we report not only that OCT represents a promising, fast developing method, which due to its characteristics fills the gap between already classical imaging investigations (MRI and ultrasounds) and new methods like two-photons microscopy but shows also potential for quantitative evaluation of the brain injuries in general [21, 23]. Nevertheless, using only synthetic statistical parameters of the detected pixel intensity as mean value, skewness and kurtosis, help us to identify the full extent of injuries but provided no comprehensive scheme for automatic detection. For this reason and taking into account the importance of these types of brain injures we try to establish the feasibility of using a much powerful mathematical tool for image analyses: artificial neural networks. In the last years, artificial neural networks show potential for diagnosis of different type of lesions, mainly because of their adaptability and excellent problem solving-oriented architecture and have been used in medical image analysis tasks with various degrees of success, with many applications in gastroenterology and tumor pathology associated with the digestive tract [24]. Our aim here is to establish the role and feasibility of OCT analysis parameters in a complex system of neural networks.

2 Material and Methods

Animals. In order to perform the study, we selected a number of 15 adult male common Sprague-Dawley rats, from the Animal Facility of the University of Medicine and Pharmacy of Craiova, aged between 19-20 months, with weights between 500-650 g. The animals were held in standard conditions of light, temperature and humidity, and had unlimited access to food and water. The environment parameters were kept constant by using an air-conditioning system. The vivarium has a cyclical lighting of 12 hours and the cages were standard sizes accommodating each two rats. For performing the experiment, we obtained the approval of the Ethics Board of the University of Medicine and Pharmacy of Craiova, according to the European Council Directive 11.24.1986 (86/609/CEE), the European Convention regarding vertebrate animal protection (2005) and Govern Ordinance No. 37/02.02.2002.

Surgery. In order to perform stroke experimental model, we induced anesthesia using a intraperitoneally administration of a mixture of xylazine hydrochloride (Narcoxyl vet, 20 mg/mL solution, Intervet, Netherlands), 10 mg/kg BW and ketamine hydrochloride (Ketamine powder 100 mg, Franciuos, the Netherlands), 90 mg/kg BW. We have used transcranial reversible (90 minutes) occlusion of the middle cerebral artery (MCAO) experimental model, which requires transient interruption of blood flow through this artery, as previously described [23] together with the bilateral, reversible clipping of the both common carotid arteries. As a result we obtain a drop of 20% from the MCA blood flow in middle cerebral artery, with the possibility to induce brain ischemia. The body temperature was maintained as close as possible to 37^oC, and arterial blood pressure, blood gas (oxygen and carbon dioxide) and serum glucose levels were determined throughout the intervention. Perfusion. After a period of four weeks, the animals were anesthetized with the same method and after heart was exposed, a flexure was introduced into the left ventricle, pumping 200 ml of saline solution (0.9% NaCl) with a pressure of 140 mmHg.

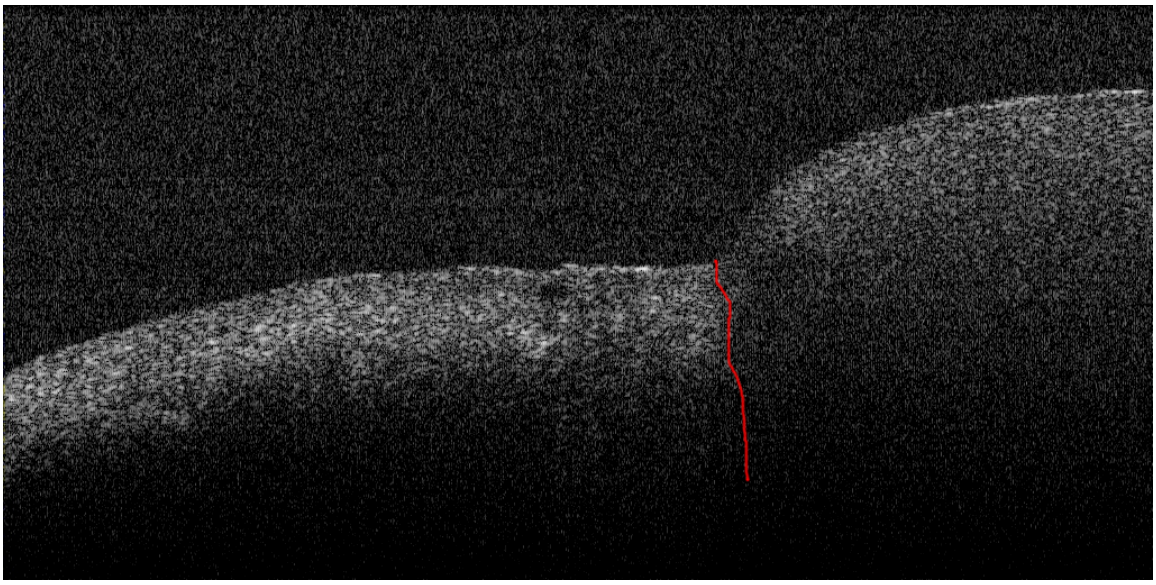

Figure 1: Optical coherence tomography image of a rat brain, 28 days after middle cerebral artery occlusion induced stroke, coronal sections 2 mm depth and 5 mm width, at frontoparietal level. Necrotic cortex tissue is easily identified (to the left of the red line) comparing with the normal tissue (to the right to the red line)

The perfusion with saline solution was immediately followed by perfusion with a solution of 4% paraformaldehyde (PFA) 5x in phosphate buffer (5xPB) for fixing tissues. After perfusion, brain was collected and placed in paraformaldehyde solution prior to OCT investigations.

Optical coherence tomography imaging. For OCT imaging we used a system provided by THORLABS (OCT1300SS), powered by a swept laser source with central wavelength of 1325 nm and a spectral bandwidth of 100 nm, with an average power of 12 mW. We investigate the affected ischemic hemisphere, including both, healthy and injured tissue, sampling coronary pictures in width of 5 mm, a distance of 3 mm and a depth of 2 mm. Acquisition was performed over a volume of 5 mm x 3 mm x 2 mm for each sample. Intact brains were investigated with optical coherence tomography and the obtained images were analyzed.

Image analysis. We have divided each stroke image into two sections; one area of interest comprised the stroke zone and one corresponded to the normal texture of the image (Figure 1). For a better characterization and discrimination of normal texture from stroke area we also used picture only with unaffected tissue (Figure 2). We then performed the imaging test in parallel and trained a neural network with the parameters provided by the test. The artificial neural network (ANN) was developed in MATLAB (MathWorks, USA) and consists of input and output layers with one hidden layer of neurons in-between for processing functions (Figure 3). The training phase used the feed-forward back propagation algorithm, already implemented in the software. The extensive image set was randomly divided between training, testing and validation. The neural network analyzed each image pixel by pixel using an automated method for comparing the similarity of two neighboring pixels (near-pixel approximation). This method has good results for grayscale images, where it can establish the intensity of an area depending on adjacent ones. For image analysis, we used a model based on the Gray Level Co-occurrence Matrix (GLCM) model proposed by Haralick [25], the correlation parameter being adjusted as described

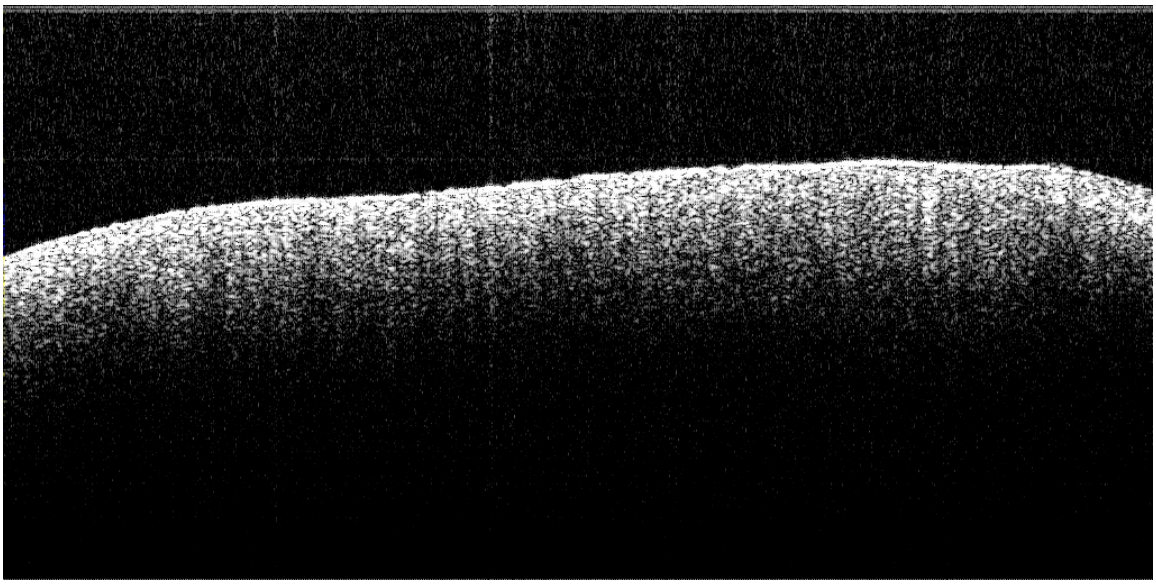

Figure 2: Optical coherence tomography image of a rat normal brain, coronal sections 2 mm depth and 5 mm width, at frontoparietal level. Normal cortex is identified

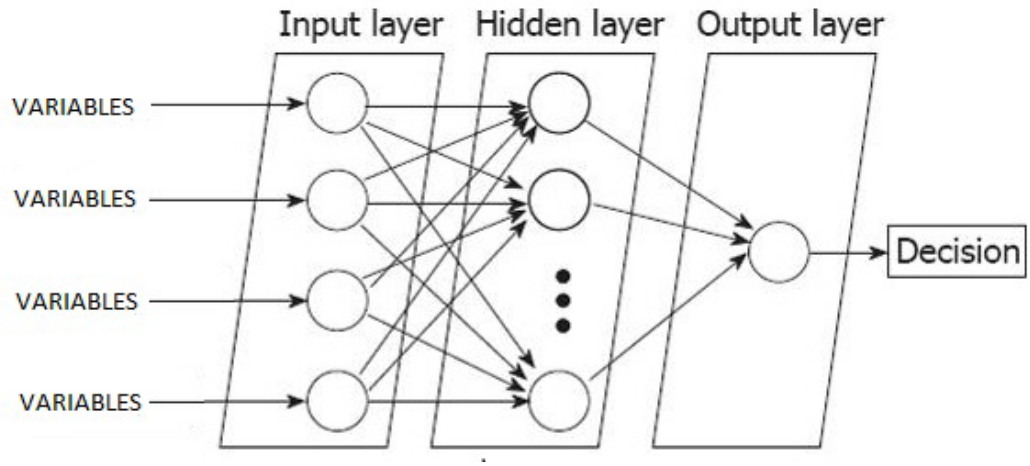

Figure 3: Graphical representation of an ANN. The variables are imputed to corresponding neurons in the first layer of the ANN, which in turn send the data to all neurons of the hidden layer. The neurons in this intermediate layer establish an importance value for the output layer, which presents the user with a result, classifying the image into one category (stroke or normal tissue)

by Walker [26]. This model was implemented in the "Texture analyzer" plug-in (Cabrera, USA) developed for the freeware software application ImageJ (Bethesda, USA). We calculated three texture descriptors: contrast, the correlation coefficient and the coefficient of entropy, for each set of textures chosen as positive classifiers (stroke areas), as well as normal areas of interest (AOIs). Contrast is used as a measure for evaluating the difference in brightness and grayscale between adjacent pixels in each image; correlation coefficient measures the correlation pairs of pixels according to the grayscale levels, and entropy is a parameter that evaluates how random is the distribution grayscale levels in the picture. The texture of four axes analyzed from a pixel as the center (0^o, 45^o, 90^o and 135^o, respectively), forming the matrix adjacent to each. Mathematical and statistical analyses were performed using ORIGIN 8 and GraphPad 5 software. The ANN was trained as to which image corresponds to stroke and which is normal, then blinded to the testing and validation sets.

3 Results and Discussions

There were reported a series of morphological and pathophysiological changes that occurs after ischemia, in the adult brain of rodents, which are complex [23], including fragmentation and condensation of chromatin, apoptosis [27] or different types of necrosis [28, 29]. All these changes were observed first in the core of the stroke, as well as in the surrounding tissue, if reperfusion is not restored efficiently (strokes penumbra). As was reported previously [23, 30], it is now accepted that cerebral ischemia can generate the death of all cells (neurons, microglia, astrocytes, endothelial cells) presented in the affected area of brain. All these changes can modify the normal architecture of the nervous tissue, which can be observed with histological and imaging techniques, including OCT, consequently of the modifications of scatter properties of the incoming light. As early reported [23], a clear distinction between the normal and affected regions inside the rat ischemic brain is possible. Nevertheless, for an easy, more accurate and rapid diagnosis, a recognition assisted by ANN can be more efficient. Also, distinguishing characteristics between different regions evaluated with the help of ANN inside the stroke area may offer, in connection with other types of investigation, valid information regarding the undergoing physiological and physiopathological processes. Analyzing the images, using arrays of GLCMs, we obtained a low variability within each group of values for each particular situation ($p < 0.05$; coefficients variation < 0.3). Thus, we have validated the reproducibility of the method for all cases studied. For contrast images we obtained lower ranges, compared to normal aspects, where gray scale differences were more pronounced ($p < 0.001$). Entropy values were different for each individual pair of AOIs ($p < 0.001$). The degree of disorganization of the texture was different for all pairs of ROIs ($p < 0.05$). The ANN model correctly classified 92% of the testing set, after successful training of 12 epochs. The system misidentified 4% of the images as being strokes whereas the areas corresponded to normal aspects; 4% of all images were incorrectly identified as normal cortex.

4 Conclusion

In conclusion, neural network analysis of stroke OCT images seems to be a promising technique for fast and reliable recognition of the stroke areas. Future studies and better

correlation of the structure and mathematical models of the ANN with ongoing processes and mechanisms inside the injured area are needed to fully validate this study. Nevertheless it is important to underline that our implementation could discriminate in a high rate between normal and ischemic tissue and we believe that association between OCT investigations and ANN has a potential to be applied in the experimental and clinical field of neuroscience.

Acknowledgements

All the authors have equally contributed to the study. C.T. Streba and S.L. Georgescu were responsible for the ANN set up and the mathematical analyses of the parameters; E. Osiac, M. Jigău and MA Dinu were responsible for the OCT experiments and results, T.A. Bălşeanu, V.C. Dinescu and B. Cătălin were responsible for the medical part (preparation of the animals, inducing stroke and medical confirmation of the damage area).

References

[1] Huang D, Swanson EA, Lin CP, Schuman JS, Stinson WG, Chang W, Hee MR, Flotte T, Gregory K, Puliafito CA, Fujimoto JG, Optical coherence tomography, Science, 1991, **254**:1178–1181, doi:10.1126/science.1957169.

[2] Toth CA, Narayan DG, Boppart SA, Hee MR, Fujimoto JG, Birngruber R, Cain CP, DiCarlo CD, Roach WP., A comparison of retinal morphology viewed by optical coherence tomography and by light microscopy, Arch Ophthalmol. 1997 Nov; **115**(11):1425-1428.

[3] Brezinski ME, Tearney GJ, Bouma BE, Optical coherence tomography for optical biopsy: properties and demonstration of vascular pathology, Circulation, 1996, **93**:1206–1213

[4] Huang D, Swanson EA, Lin CP, Schuman JS, Stinson WG, Chang W, Hee MR, Flotte T, Gregory K, Puliafito CA, Fujimoto JG, Optical coherence tomography, Science, 1991, **254**:1178–1181.

[5] Swanson EA, Izatt JA, Hee MR, Huang D, Lin CP, Schuman JS, Puliafito CA, Fujimoto JG, In vivo retinal imaging by optical coherence tomography, Opt Lett, 1993, **18**(21):1864-1866.

[6] Brezinski ME, Tearney GJ, Bouma BE, Optical coherence tomography for optical biopsy: properties and demonstration of vascular pathology, Circulation, 1996, **93**:1206–1213.

[7] Brezinski ME, Optical Coherence Tomography: Principles and Applications, Academic Press, Burlington, 2006.

[8] Swanson EA, Izatt JA, Hee MR, Huang D, Lin CP, Schuman JS, Puliafito CA, Fujimoto JG, In vivo retinal imaging by optical coherence tomography, Opt Lett, 1993, **18**(21):1864-1866.

[9] Fercher AF, Hitzenberger CK, Drexler W, Kamp G, Sattmann H, In Vivo Optical Coherence Tomography, Am Journal Ophthal, 1993, **116**:113–114.

[10] Fénolland JR, Puech M, Baudouin C, Labbé A, Imaging of the iridocorneal angle in glaucoma, J Fr Ophtalmol, 2013, **36**(4):378-383

[11] Isenberg G, Sivak MV, Gastrointestinal Optical Coherence Tomography, Techniques in Gastrointestinal Endoscopy, 2003, **5**(2): 94-101.

[12] Chen Y, Aguirre AD, Hsiung PL, Huang SW, Mashimo H, Schmitt JM, Fujimoto JG, Effects of axial resolution improvement on optical coherence tomography (OCT) imaging of gastrointestinal tissues, Optics Express, 2008, **16**(4):2469-2485.

[13] Osiac E, Săftoiu A, Gheonea DI, Mandrila I, Angelescu R, Optical coherence tomography and Doppler optical coherence tomography in the gastrointestinal tract, World J Gastroenterol, 2011, **17**(1):15–20.

[14] Zhang J, Zhongping C, Isenberg G, Gastrointestinal Optical Coherence Tomography: Clinical Applications, Limitations, and Research Priorities, Gastrointest Endoscopy Clin N Am, 2009, **19**:243–259.

[15] Welzel J, Optical coherence tomography in dermatology: a review, Skin Research and Technology, 2001, **7**:1–9.

[16] Boppart SA, Brezinski ME, Pitris C, Fujimoto JG, Optical Coherence Tomography for Neurosurgical Imaging of Human Intracortical Melanoma, Neurosurgery, 1998, **43**:834-841.

[17] Zhang K, Huang Y, Pradilla G, Tyler B, Kang JU, Real-time intraoperative full-range complex FD-OCT guided cerebral blood vessel identification and brain tumor resection in neurosurgery, Proc of SPIE, 2011, **78833Y**:1-8.

[18] Srinivasan VJ, Radhakrishnan H, Jiang JY, Barry S, Cable AE, Optical coherence microscopy for deep tissue imaging of the cerebral cortex with intrinsic contrast, Optics Express, 2012, **20**:2220–2239.

[19] Radhakrishnan H, Srinivasan VJ, Compartment-resolved imaging of cortical functional hyperemia with OCT angiography, Biomedical Optics Express, 2013, **4**(8):1255-1268

[20] Srinivasan VJ, Mandeville ET, Can A, Blasi F, Climov M, Daneshmand A, Lee JH, Yu E, Radhakrishnan H, Lo EH, Sakadzic´S, Eikermann-Haerter K, Ayata C, Multiparametric, Longitudinal Optical Coherence Tomography Imaging Reveals Acute Injury and Chronic Recovery in Experimental Ischemic Stroke, PLoS ONE, 2013, **8**(8):e71478.

[21] Osiac E, Balseanu TA, Catalin B, Mogoanta L, Gheonea C, Dinescu SN, Albu CA, Cotoi BV, Sfredel V, Optical coherence tomography as a promising imaging tool for brain investigations, Rom J Morphol Embryol, 2014, **55**(2 suppl), 507-512.

[22] Burton KR, Perlis N, Aviv RI, Moody AR, Kapral MK, Krahn MD, Laupacis A, Systematic review, critical appraisal, and analysis of the quality of economic evaluations in stroke imaging, Stroke, 2014, **45**(3):807-814.

[23] Osiac E, Bălşeanu TA, Mogoantă L, Gheonea DI, Pirici I, Iancău M, Mitran SI, Albu CV, Cătălin B, Sfredel V., Optical coherence tomography investigation of ischemic stroke inside a rodent model, Rom J Morphol Embryol, 2014, **55**(3), 767-772

[24] Streba CT, Ionescu M, Gheonea DI, Sandulescu L, Ciurea T, Saftoiu A, Vere CC, Rogoveanu I., Contrast-enhanced ultrasonography parameters in neural network diagnosis of liver tumors, World J Gastroenterol, 2012, **18**(32):4427-4434.

[25] R.M. Haralick, K. Shanmugam, I. Dinstein, Textural Features for Image Classification, IEEE Transactions on Systems, Man, and Cybernetics, 1973, **3**(6), 610–621.

[26] R.F. Walker, P.T. Jackway, D. Longstaff, Genetic Algorithm Optimization of Adaptive Multi-Scale GLCM Features, International Journal on Pattern Recognition and Artificial Intelligence, 2003, **17**(1), 17–39.

[27] Charriaut-Marlangue C, Richard E, Ben-Ari Y, DNA damage and DNA damage-inducible protein Gadd45 following ischemia in the P7 neonatal rat, Brain Res Dev Brain Res, 1999, **116**(2):133-140.

[28] Kessler Ch, Junker H, Bălşeanu TA, Oprea B, Pirici D, Mogoantă L, Popa-Wagner A, Annexin A3 expression after stroke in the aged rat brain, Rom J Morphol Embryol. 2008;**49**(1):27-35.

[29] Mogoantă L, Pirici D, Pop OT, Bălşeanu AT, Rolea E, Dahnovici RM, Study of vascular microdensity in areas of cerebral ischemia on experimental model, Rom J Morphol Embryol. 2010; **51**(4):725-31.

[30] Wieloch T, Molecular Mechanisms Of Ischemic Brain Damage. In: Edvinsson L and Krause DN (ed), Cerebral Blood Flow and Metabolism, Second Edition, Lippincot Williams & Wilkins, Philadelphia, 2001, 423-451